LA-UR- 08-5628

Approved for public release; distribution is unlimited.

Title:	Estimating the Impact of vaccination in Acute SHIV/SIV Infection.
Author(s):	R. Ribeiro, Z # 171295, T-10/T-Division
Intended for:	Journal of Virology

Form 836 (7/06)

Estimating the Impact of Vaccination in Acute SHIV/SIV Infection

Janka Petravic[1]

Ruy M. Ribeiro[2]

Danilo R. Casimiro[3]

Joseph J. Mattapallil[4]

Mario Roederer[5]

John W. Shiver[3]

Miles P. Davenport[1*]

[1] Complex Systems in Biology Group, Centre for Vascular Research, University of New South Wales 2052, Australia

[2] Theoretical Biology and Biophysics, Los Alamos National Laboratory, Los Alamos NM 87545

[3] Merck Research Laboratories, West Point PA

[4] Department of Microbiology and Immunology, Uniformed Services University of Health Sciences, Bethesda, MD 20824

[5] ImmunoTechnology Section, NIAID, NIH, Bethesda, MD 20892

Abstract:

The dynamics of HIV infection have been studied in humans and in a variety of animal models. The standard model of infection has been used to estimate the basic reproductive ratio (R_0) of the virus, calculated from the growth rate of virus in acute infection. This method has not been useful in studying the effects of vaccination, since, in the vaccines developed so far, early growth rates of virus do not differ between control and vaccinated animals. Here, we use the standard model of viral dynamics to derive the reproductive ratio from the peak viral load and nadir of target cell numbers in acute infection. We apply this method to data from studies of vaccination in SHIV and SIV infection and demonstrate that vaccination can reduce the reproductive ratio by 2.3 and 2 fold respectively. This method allows the comparison of vaccination efficacy amongst different viral strains and animal models *in vivo*.

Introduction

Human Immunodeficiency Virus (HIV) infects approximately 0.5% of the world population, and is a major cause of morbidity and mortality worldwide. A vaccine for HIV is urgently required, and a variety of vaccine modalities have been tested in animal models of infection. A number of these studies have shown protection in monkey models of infection, although the ability of the vaccine to protect appears to vary with the viral strain and animal model used (8). The recent failure of a large vaccine study in humans (1) suggests that further understanding of the basic dynamics of infection and impact of vaccination are required, in order to understand the variable efficacy of vaccination in different infections.

The initial ability of HIV to propagate within the host is determined by the abundance of target cells (e.g. CD4+ T lymphocytes) it can infect in order to produce progeny, by the replicative capacity of the virus and by how cytopathic it is to infected cells. At later stages of the disease, in addition to changes in the target cell availability, there may also be changes in virus-specific properties such as the ability of virus to reproduce and the survival of productively infected cells as a result of changes in immune pressure and viral evolution. These parameters may be variable amongst individuals and within one individual over time, and affect the impact of vaccination. In order to compare the efficacy of vaccination strategies, we need a quantitative measure of the factors that influence virus replication.

In this work we focus on the basic reproductive ratio as a measure of vaccine efficacy in the acute phase of infection. In epidemiology, the basic reproductive ratio R_0 measures the potential of spread of an epidemic, and is defined as the average number of people infected by one infected individual in a susceptible population. If this number is below one, the disease will not spread in a population. Therefore, the knowledge of R_0 allows one to estimate the fraction of population that needs to be vaccinated in order to eradicate the disease. Analogously, in host-pathogen dynamics the basic reproductive ratio is defined as the number of infected cells generated by one infected cell during its lifetime at the start of infection, i.e. before any depletion of target cells. In order for the infection to spread within the host, this number has to be larger than one; otherwise the infection will be cleared before it has a chance to spread. The basic reproductive ratio will depend on the ability of virus to infect cells ("infectivity"), on the production rate of virions by infected cells, on the lifetime of

infected cells and on the rate at which free virus is cleared. The aim of vaccines is therefore to create virus-specific immunity that changes any of these parameters and thus decreases the basic reproductive ratio of the virus, preferably below one (so infection does not spread beyond the initially infected cells). The importance of R_0 in HIV vaccination, in order to assess how much protection a particular vaccine can achieve, has been stressed previously (11). In particular, it could be a very useful and common standard to compare different vaccination protocols.

The basic reproductive ratio can be determined from the rate of exponential growth of virus in the initial period during which the target cell levels are almost constant (14, 19, 27). However, in monkeys infected with the same type of simian immunodeficiency virus there is in fact very little variation in the basic reproductive ratio determined from the initial exponential growth, independently of vaccination, despite the variety of outcomes later in infection. Different factors identified as possible predictors of disease progression (27), such as the peak viral load, target cell nadir, decay rate of virus following peak viremia, set point viral load and chronic target cell levels,, correlate poorly or not at all with the differences in reproductive ratio determined from the primary exponential growth phase (27). In particular, it is not possible to assess the efficacy of cytotoxic T-lymphocyte (CTL) based vaccines on the basis of the basic reproductive ratio, because there is no effect of vaccination on viral growth before approximately 10 days post infection, which is at the end of the exponential growth period (4, 6).

We have recently shown the existence of a strong correlation between the viral load at peak and the target cell depletion in the acute phase (7, 29). Using this correlation, one can show that vaccination results in the reduction of peak viral load and of acute CD4+ T-cell depletion, thus improving the chronic phase prognosis.

The dependence of the nadir in CD4+ T-cell depletion on the viral peak can be obtained from the standard model of virus dynamics (7, 29). Here we show that this relationship between the viral peak and the number of target cells one week after the peak (corresponding approximately to the minimum of target cells in primary infection) is parameterized by the basic reproductive ratio of the virus. In other words, the decrease in peak viral load leads to the less target cell depletion at nadir, and both are a consequence of lower basic reproductive ratio. Thus, we can in principle determine the basic reproductive ratio from experimental data of the viral peak and target cell nadir. We show that this relationship is indeed supported by experimental

data from CXCR4-tropic Simian Human Immunodeficiency Virus (SHIV) infection (for viral loads and CD4+ T-cell counts in peripheral blood), and for CCR5-tropic Simian Immunodeficiency Virus (SIV) infection data (for plasma viral loads and memory CD4+ T-cell depletion in the gut).

We show that the reproductive ratio estimated from the viral peak and the target cell nadir, which we call the "reproductive ratio at the peak", is significantly lower than the basic reproductive ratio estimated from the exponential growth. In addition, we find that in vaccinated animals the reproductive ratio at the peak is on average two-fold lower than in control animals. We attribute this difference to the cellular immune response appearing before the peak viral load, around day 10 of infection, and changing the properties of the virus and infected cells dynamics (e.g. decreasing lifetime of infected cells through cytolytic function of CTLs, or changing infectivity or virus production through release of cytokines). Thus, we propose that the "reproductive ratio at the peak", a measurement that includes information both on viral peak and target cell nadir, can be useful as a standard to compare vaccine protocols.

Materials and methods

In the CXCR4-tropic virus study, 35 rhesus macaques (*Macaca mulatta*) were vaccinated with a variety of regimens, consisting of SIV gag containing plasmid DNA (with different adjuvants), modified vaccinia Ankara, and adenovirus type 5 vectors, as previously reported (25). Animals were challenged intravenously at 6 weeks (study A) or at 12 weeks (study B) after the final boost with 50% monkey infectious doses of SHIV-89.6P. Viral loads and CD4+ T-cell counts were monitored in peripheral blood every 2 to 4 days until 4 weeks after infection and then weekly. The results of the two studies were merged together for the purpose of this work.

In the CCR5-tropic virus study, 20 rhesus macaques were challenged intravenously with 100 monkey infectious doses of uncloned SIVmac251. Six of these animals received prior vaccination with plasmid DNA encoding SIV envelope, Gag and Pol, and were boosted with recombinant adenovirus encoding the same antigens. Plasma and jejunum tissue samples were collected at various time points by biopsy or at necropsy, and tissue CD4+ T-cell percentages and plasma viral loads were determined (17, 18).

Results

Reproductive ratio in the initial exponential growth phase of disease

The standard model of virus dynamics (15, 20),

$$\frac{dT}{dt} = \lambda - d_T T - \beta VT \qquad \text{Eq. 1}$$

$$\frac{dI}{dt} = \beta VT - \delta I \qquad \text{Eq. 2}$$

$$\frac{dV}{dt} = pI - cV \qquad \text{Eq. 3}$$

describes the relationships between the change in the number of uninfected cells T that are targets for the virus, infected cells I and free virus particles V in a given volume of blood or tissue. The parameters λ, the production rate of new target cells, and d_T, the loss rate of uninfected cells, describe the disease-free target cell dynamics. The disease-free equilibrium number of target cells is equal to $T_0=\lambda/d_T$. The infectivity β characterizes the probability of a virus particle infecting a target cell, and δ is the death rate of infected cells, $\delta >> d_T$. Free virus is produced by infected cells at rate p and is cleared at rate c. In this model, the immune response is assumed to be constant and its effects are contained in the virus parameters δ, c, β and p. All the parameters are assumed to be constant in time (see also [Cite Stafford et al JTB]). The basic reproductive ratio R_0 for this model is (15, 20)

$$R_0 = T_0 \frac{\beta p}{\delta c}. \qquad \text{Eq. 4}$$

The virus infection can spread only if $R_0>1$. In this case, viral load generally increases to the peak and then decays, in order to finally reach the steady-state value V^*. Target cells drop to the minimum, then partly recover and settle at the steady-state value $T^*= T_0/R_0$. This standard model has been used to investigate different aspects of HIV/SIV/SHIV infection, such as the turnover of infected cells (7, 12, 28), clearance rate of virus (22) and 'burst size' of infected cells (3, 13).

The basic reproductive ratio of a virus is determined from the initial rate of exponential expansion r_0 during which the number of target cells is approximately constant (24) [cite also Nowak, J Virol and Little J Exp Med],

$$\frac{1}{V}\frac{dV}{dt} \equiv r_0 \approx \delta(R_0 - 1). \qquad \text{Eq. 5}$$

In Figure 1 we show viral load data during the first weeks of infection from the Shiver *et al.* study (25), in which 21 out of 35 rhesus macaques were vaccinated with 7 different SIV gag–containing vaccines, and all 35 were challenged intravenously with CXCR4-tropic SHIV-89.6P. Black lines represent viral load in the control animals and red lines represent vaccinated animals. The initial exponential growth rate and the decay rate of virus after the peak are remarkably similar between monkeys, irrespective of whether they were vaccinated or not. The statistical analysis results are summarized in Table 1.

If we use the rate of decline of viral load after the peak as an estimate of the death rate of infected cells, δ, in each animal, we obtain from the early exponential growth rate that R_0=2.4 for vaccinated animals (95% confidence interval (CI) 2.3 to 2.6) and almost the same R_0=2.5 for control animals (95% CI 2.3 to 2.7). The two values are not statistically different (Mann-Whitney p=0.391).

On the basis of the similarity in virus growth and decay rates between control and vaccinated animals, we (4, 6) and others (23) concluded that the cellular (CD8+ T-cell) immune response does not emerge before at least 10 days post-infection (reviewed in (5)). This is why it has not been possible to asses the effects of vaccination from the reproductive ratio of the virus calculated from its growth rate within this initial period of 10 days.

Eq. **5** considerably underestimates R_0 because it neglects the delay between the time when a cell becomes infected and the time when it starts producing the virus. In a model with a fixed intracellular delay τ (and assuming that all infected cells survive the delay period) (10), R_0 is found from the initial growth rate as (15, 24)

$$R_0 = (1 + r_0/\delta)e^{r_0\tau}. \qquad \text{Eq. 6}$$

With a delay of 1 day (21), we obtain R_0=9.9 for vaccinated animals (95% CI 8.6 to 11) and R_0=11 for control animals (95% CI 8.6 to 12), again not different for the two groups, and consistent with previous studies of the basic reproductive ratio in SIV infection (19).

Virus peak and target cell nadir in the standard model of virus dynamics

We would like to calculate the peak in viral load and the nadir in target cells. This is quite difficult for the standard model (Eqs. 1-3). However, before infection target cells are approximately in equilibrium, which implies that $\lambda - d_T T_0 \approx 0$. Thus,

up to the peak of infection, while there is very little depletion in T_0 (Fig. 2), we can neglect those two terms in Eq. **1** because they balance each other. After the peak of infection, and as long as V and T are not too small, $\beta VT >> \lambda - d_T T$, and thus again we can neglect the latter two terms. That is, we can simplify the standard model to (7),

$$\frac{dT}{dt} = -\beta VT, \qquad \text{Eq. 7}$$

$$\frac{dI}{dt} = \beta VT - \delta I, \qquad \text{Eq. 8}$$

$$\frac{dV}{dt} = pI - cV. \qquad \text{Eq. 9}$$

In this reduced model, viral load always vanishes at long times (i.e. infection is always cleared if there is no natural loss and replacement of target cells), with target cells steadily declining towards a low steady-state value T_{min}. However, we can further justify our approximation by noting that the profile of viral load and target cell dynamics during primary infection (up to the target cell nadir, days 18-20 in Fig. 2) is only mildly affected. As expected, the exponential growth rate of the virus is the same as in the full standard model, and viral load has a maximum V_P, with a value very close to the peak of the standard model (Figure 2a).

Figure 2 also shows that the steady state target cell number T_{min} in the reduced model (full line in Figure 2b) is slightly lower, but still a very good approximation for the uninfected target cell nadir of the standard model Eq. **1**-Eq. 3 (dashed line in Figure 2b) for the parameters λ=10cells/μL/day, d_T=0.01/day (26) usually attributed to CD4+ T-cells in HIV/SIV/SHIV infection. The condition for Eq. 7 to be a good approximation to the full model, that is $\beta VT >> \lambda - d_T T$, is only violated very close to the nadir of target cells, as viral load decreases, and that is why we obtain a good estimate of the nadir from this approximation. This is true whenever λ is relatively small.

Instead of uninfected target cells, the quantity that is usually measured experimentally is the total number of uninfected and infected cells ($T+I$). Figure 2b shows that the minimum of the total T cell number (the dotted line) is again very close to the minimum of target cells (dashed line). Therefore we can safely use the steady state number of uninfected cells from the reduced model T_{min} as an estimate of the measured total target cell minimum.

An advantage of the reduced system Eq. 7-Eq. 9 is that one can estimate V_P and T_{min} analytically. We shall use the analytical results as estimates for the viral peak and the target cell nadir in the full standard model.

The basic reproductive ratio of the reduced model, R_0, is still given by Eq. 4 (with T_0 being an arbitrary initial target cell number). The peak of viremia, as a function of R_0, is (see Appendix for derivation)

$$V_P = \frac{\delta}{\beta} R_0 \left(1 - \frac{1}{R_0} - \frac{\ln R_0}{R_0} \right), \quad \text{Eq. 10}$$

valid for the reduced model (Eq. 7-Eq. 9) and a good approximation for the standard model, with low target cell replacement and loss (Eq. **1**-Eq. 3).

T_{min} is found as the solution of the equation (see Appendix)

$$\frac{T_{\min}}{T_0} - \frac{1}{R_0} \ln \frac{T_{\min}}{T_0} = 1. \quad \text{Eq. 11}$$

The fraction of uninfected target cells at the nadir in the full standard model, approximately equal to T_{min}/T_0 in Eq. 11, depends only on the basic reproductive ratio R_0. The solution is illustrated in Figure 3. For R_0>5, the value of T_{min}/T_0 is practically zero and the depletion at nadir is almost 100%. In Figure 3 we plotted both T_{min}/T_0 (the ratio at the target cell nadir) and T^*/T_0 (the ratio in chronic infection, i.e. in the steady state, given by $1/R_0$) as functions of R_0, showing that T_{min} is always (for all R_0) less than the steady-state target cell count T^*.

Relationship between the virus peak and the target cell nadir

In the context of acute infection, i.e. the time between the virus peak and the target cell nadir, we shall call the expression in Eq. 4 the reproductive ratio at the peak (and use the symbol R_P) instead of the basic reproductive ratio, in order to stress that the parameter values in this period may have changed from those of initial infection. Thus, one should replace the symbol R_0 by R_P in Eq. 10 and Eq. 11. For very low target cell replacement rate λ and loss rate d_T, the depletion at the target cell nadir $D=1-T_{min}/T_0$ (from Eq. 11) depends only on the reproductive ratio at the peak R_P, since this is the only free parameter in the equation. The peak viral load (Eq. 10) depends on R_P, and in addition on the ratio δ/β. This means that, for viruses with different characteristic infectivities, β, or different cytotoxicities and cellular immune responses resulting in different loss rates of infected cells, δ, the relationship between

the virus peak and the target cell minimum will be described by a family of parallel sigmoid curves (Figure 4a). R_P varies along each curve with the characteristic ratio δ/β. Increases in infectivity shift the curve to the left, while decreases in infectivity shift it to the right.

Reducing the reproductive ratio at the peak for a given virus decreases the peak viral load. The reduction of peak by, say, 0.5 log will have little effect on target cell depletion for very high viral loads (when R_P is high – plateau at nearly 100% depletion in Figure 4), but the same reduction can significantly reduce depletion and change the prognosis for lower viral loads (Figure 4b).

As an illustration, we present the SHIV-89.6P data (25) for the peak of virus and the depletion at the CD4+ T-cell minimum. The advantage of considering a CXCR4-tropic virus is that it infects "all" CD4+ T-cells, so that the target pool in peripheral blood is well-defined and can be measured. In addition, for the total number of CD4+ T-cells, it is safe to assume that the net replacement rate λ from the external source (thymus) and, consequently, the loss rate d_T are slow (i.e. that less than 1% of the normal uninfected CD4+ T-cell number is replaced from the thymus per day).

In Figure 5a we show the measured values of depletion of CD4+ T-cells at the nadir, defined as $(1-T_{min}/T_0)\times 100\%$, against the peak viral load for control (full circles) and vaccinated (open circles) animals. The theoretical relationship between the virus peak (Eq. 10) and the CD4+ nadir (T_{min} in Eq. 11) for each value of the reproductive ratio R_P depends on δ/β. We have shown in our earlier work that δ and β do not vary much between individual monkeys, whether vaccinated or not. Briefly, the death rate of infected cells is the main determinant of the slope of viral load after the peak, and it does not differ between controls and vaccinees (Table 1 and references (4, 6)). Also, we have estimated infectivity of SHIV-89.6P in rhesus macaques on the same data set, and found that there is no significant difference between vaccinated and unvaccinated animals (7). As explained in Figure 4a, the shape of the theoretical sigmoid curve $D(V_P)$ cannot be changed by fitting, since it is parametrized only by R_0. It is universal for all diseases that are well described by the standard model, with small replacement and loss rates of target cells. However, by shifting the curve along the x-axis, we can determine the best-fit value of the factor δ/β that minimizes the sum-of-squares deviation of experimental data from the

theoretical curve (see Figure 4a). Since the quantities described by both axes have errors, the squared deviation of each point is defined as the sum of squares of the deviations in x and y-direction from the closest point on the theoretical curve (a form of type 2 regression). We found the best fit value of $\log(\delta/\beta)=7.53$ ($\delta/\beta=3.39\times10^7$ copies/mL) with confidence interval 7.45 to 7.65 found by bootstrapping. The correlation coefficient was $r^2=0.985$.

In our previous work (7), we estimated infectivity from the relationship between peak viral load and the number of CD4+ T-cells one week after the peak, using the experimental viral load timeline and the first two equations of the reduced model Eq. 7 and Eq. 8. The procedure required the advance knowledge of the death rate of infected cells δ, which we estimated from the maximum decay rate of viral load after the peak as $\delta=0.84$/day. This led to the best fit average infectivity of $\beta=4.4\times10^{-8}$ mL copy^{-1} day^{-1} (95% confidence interval between 3.4 and 5.6×10^{-8} mL copy^{-1} day^{-1}). Our present estimate of $\delta/\beta=3.39\times10^7$ copies/mL with $\delta=0.84$/day would give a lower best fit infectivity of 2.48×10^{-8} mL copy^{-1} day^{-1} for the same death rate of infected cells. However, since the death rate of infected cells used in the previous work was the minimum estimate of the actual death rate, it is possible that both δ and our best fit infectivity are higher.

Analyzing infection by CCR5-tropic viruses is complicated because the number of target cells (CCR5+ CD4+ T-cells) is more difficult to measure. However, in the gastrointestinal tract most CD4+ T-cells express CCR5 coreceptor, so that most gut CD4+ T-cells are targets for CCR5-tropic viruses. In recent studies, Mattapallil *et al* [24,25] measured CD4+ depletion in the jejunum in 20 rhesus macaques infected with CCR5-tropic SIV_{mac251}, 6 of which were previously vaccinated.

Nine animals were euthanized before the viral load reached the first peak, so they could not be analysed. Figure 5b contains data points from the remaining 11 animals (7 control animals – solid circles and 4 vaccinated animals – open circles). The longitudinal data for each animal contains only three results of gut biopsies with percentages of CD4+ T-cells out of all CD3+ lymphocytes, and the lowest percentage was always the last point. We considered this point to be close to the target cell nadir.

We assumed slow replacement λ of lost gut memory cells. Our justification for this assumption is that we have recently demonstrated (29) that the CD4 depletion one week after the virus peak in the gut of the monkeys from this study is related to

the virus peak in a similar way to that seen in CD4 depletion in SHIV infection in peripheral blood. One possible explanation for slow gut replacement is that the size of the gut (and mucosal tissue) compartment is so large that the increase in production of tissue-homing CD4 T cells makes little difference. Another is that most of the new memory cells circulate and only a small portion stays in the gut as replacement.

The decay rate of SIV_{mac251}-infected cells has been independently estimated as δ=1.49/day (2). By means of the same procedure using Eq. 7,

Eq. 8 and experimental viral load, we then estimated the infectivity as $\beta=1.45\times10^{-7}$ mL copy^{-1} day^{-1}, so that $\delta\beta=1.02\times10^{7}$. The dashed line in Figure 5 shows the theoretical dependence of memory CD4+ T-cell nadir on virus peak given by Eq. 10 and Eq. 11 for this value of $\delta\beta$.

The full line corresponds to the value of $\log(\delta\beta)=7.20$ ($\delta\beta=1.58\times10^{7}$ copies/mL), which minimizes the sum-of-squares deviation of experimental data from the theoretical curve (C.I. for $\log(\delta\beta)$ is from 7.09 to 7.59, correlation coefficient r^2=0.874). The scatter of the experimental points around the theoretical curve is much larger than for SHIV infection in Figure 5a. One reason for the larger scatter is the infrequent sampling in the longitudinal data (each animal only had one biopsy before challenge, one post challenge, and a necropsy), which probably caused imprecision in the estimates of the minimum. One would need in principle several samples in the 2-3 week period after the peak in order to correctly estimate the nadir. Another reason for the scatter could be that the depletion was calculated from the change in fraction of CD4+ T-cells (out of all CD3+ cells) instead of the CD4+ T-cell count used in the model. The two ways of calculating depletion would be equivalent only if the number of CD3+ lymphocytes stayed constant during the infection. The increased scatter of experimental data compared to the SHIV infection can also be observed in the curve fit in Ref. (29).

Vaccination reduces the reproductive ratio at the peak of the virus

Figure 5a shows that vaccinated animals have on average significantly lower peak viral loads (vaccinated $\log V_P$=7.19 (95% C.I. between 6.92 and 7.47); unvaccinated $\log V_P$=8.03 (95% C.I. 7.78 and 8.28; Mann-Whitney p=0.0004) and lower CD4+ T-cell depletion at minimum (vaccinated D_{min}=81.7% (95% C.I. 71.4 and 92.1%); unvaccinated D_{min}=97.4% (95% C.I. 95.2 and 99.7%); Mann-Whitney

p=0.0003), so that we expect the average reproductive ratio at the peak to be lower in vaccinated animals. The results are summarized in Figure 6.

The change of reproductive ratio from R_0 to R_P is assumed to be the result of the change of virus-dependent parameters due to the onset of cellular immunity a few days before the peak of viral load, i.e. before significant depletion of target cells. The relationship between virus peak and CD4+ T-cell nadir in SHIV-89.6P is consistent with slow replacement of uninfected cells, so that in this case depletion at nadir can be considered to be completely determined by the peak reproductive ratio R_P of the virus (Eq. 11). From the range of the nadir CD4+ T-cell depletions and peak viral loads, we can determine the range of the reproductive ratios at the peak of SHIV-89.6P in the infected animals in the Shiver et al. study [18]. In principle, nadir depletion would give an unambiguous estimate of R_P. However, the points with nearly 100% depletion at the nadir do not give a good resolution for finding R_P, since for any R_P>4.65 the predicted nadir depletion is greater than 99%. Therefore we estimate the range of R_P from the range of peak viral loads and the line of best fit in Figure 5a, assuming $\delta\beta=10^{7.53}$. The obtained range of R_P is between 1.5 and 19.2. Vaccinated animals have on average significantly lower peak reproductive ratio (Mann-Whitney p=0.0007). The peak reproductive ratio for vaccinated animals is R_P=3.81 with 95% CI between 2.3 and 4.6. For unvaccinated animals, R_P=8.87 with 95% CI between 4.8 and 11.0.

The range of R_P determined from the peak viral load depends on the best fit value of $\delta\beta$. However, the finding that it is significantly reduced by vaccination is not very sensitive to the variations in this value. For $\delta\beta=10^{7.28}$ (the estimate from ref. [8]), vaccinated animals have R_P=4.6 with 95% confidence interval between 2.8 and 6.5. For control animals, R_P=12.0 with 95% confidence interval between 6.8 and 17.2. Thus, the reproductive ratio at the peak is still significantly higher in control animals (Mann-Whitney p=0.0012).

Since the 21 animals in the Shiver study were vaccinated with 7 different types of vaccines, all we can conclude is that, in general, the effect of vaccination is to reduce the peak reproductive ratio of the virus. The amount by which R_P is reduced with respect to the average in control animals would reflect the effectiveness of a particular vaccine.

We obtained similar reduction in the reproductive ratio at the peak for SIV_{mac251} in the jejunum tissues of the macaques in the Mattapallil *et al.* study (17, 18). The vaccinated animals had R_P=1.8 and control animals had R_P=3.6, however the difference did not reach significance (Mann-Whitney p=0.073) due to the small sample size (eleven animals).

Discussion

We have shown that the relationship between the virus peak and the target cell nadir in the acute phase of the CXCR4-tropic SHIV infection and CCR5-tropic SIV infection is consistent with the standard model of virus dynamics. This relationship allowed us to estimate the decrease in reproductive capacity of the virus caused by vaccination.

The basic reproductive ratio contains all model parameters in the initial exponential growth phase of the virus. It does not reflect the effects of the cellular immune responses (or, consequently, the effects of vaccination) in primary infection, because in current vaccines these effects only become evident at the end of the early expansion period.

We have defined the reproductive ratio at the peak as the same function of the standard model parameters as in the basic reproductive ratio, but evaluated in the period between the viral peak and the CD4+ T-cells nadir. In this period, CTL response is the main factor responsible for the change of parameters. In the absence of CTL responses, the basic and the peak reproductive ratios would probably be the same (this is in principle testable in macaques with anti-CD8 treatment). However, our method cannot determine specifically which parameters have changed as a result of the CTL response, only that the compound quantity R_P has changed considerably.

We found that in both SHIV and SIV infections vaccination on average reduced the reproductive ratio at the peak between 2 and 2.5 times. This was not sufficient to clear the virus. In order to suppress the infection during the first few weeks, vaccines should decrease the reproductive ratio below unity, i.e. approximately 8-fold for SHIV and 4-fold for SIV.

We have shown that the decrease of the reproductive ratio at the peak with respect to the basic reproductive ratio simultaneously causes the peak viral load to decrease and the target cell number at nadir to increase, i.e. the two effects are

strongly correlated and have the same origin. In addition, our analysis explains why it is possible to have highly variable peak viral loads when target cells are almost completely depleted at nadir (plateau of the curve in Figure 4). The disadvantage of using the reproductive ratio at the peak as a measure of immune pressure is that the method requires the knowledge of the target cell numbers, which is straightforward to measure in blood for CXCR4-tropic viruses, but may require sampling of mucosal sites for CCR5-tropic viruses like HIV (9). With this limitation, the method would be applicable to a variety of viral infections.

Vaccination trials have been used to compare the effectiveness of different vaccines in a number of monkey species, and using a wide variety of vaccine modalities. The efficacy of different vaccines can then be ranked by comparison of their ability to preserve $CD4^+$ T cell numbers or reduce peak viral loads. Such comparisons can be at times misleading, since in viruses with a higher R_0, it is much more difficult to prevent CD4 T cell depletion than viruses with low R_0. Thus, the ideal metric for ranking vaccines would allow comparison of efficacy both within one infection model and across multiple infection models. Moreover, such a metric should also allow consideration of whether a given vaccine may be more effective in more virulent infections (with high R_0) or less virulent infections, in order to predict which will perform best in HIV. The basic reproductive ratio at peak permits such comparisons. In addition, it also has the inherent threshold of unity in its definition. The idea of reducing the basic reproductive ratio of the virus below unity by inducing specific immune response has been present in the context of HIV vaccination for a long time (11). However, we believe that we present the first method that allows to evaluate the impact of vaccination using such concept, in this case the "reproductive ratio at the peak".

Acknowledgment

This work was supported by the James S. McDonnell Foundation 21st Century Research Award/Studying Complex Systems, and the Australian National Health and Medical Research Council (NHMRC). MPD is a Sylvia and Charles Viertel Senior Medical Research Fellow. RMR was supported by grant P20-RR18754 from the National Instututes of Health (NIH)

Appendix

Derivation of Eq. 10 for virus peak

Let us assume that at the start of infection, t=0, we have initial target cell number T_0 and initial viral load V_0, with initial number of infected cells I_0=0. If the peak viral load V_P occurs at time t_P, and the target and infected cell numbers at t_P are T_P and I_P respectively, then

$$\frac{dV}{dt} = pI_P - cV_P = 0 \qquad \text{A 1}$$

leads to

$$I_P = \frac{c}{p}V_P. \qquad \text{A 2}$$

If we assume that V and I peak at the same time, which is true when $c>>\delta$, then from

$$\frac{dI}{dt} = \beta V_P T_P - \delta I_P = 0 \qquad \text{A 3}$$

follows that

$$T_P \approx \frac{\delta c}{\beta p} = T^* = \frac{T_0}{R_0} \qquad \text{A 4}$$

where T^* is the steady-state target cell number in the full standard model, Eq. 1-Eq. 3. The lag between the peak of infected cells and viral load becomes negligible in the limit $\delta<<c$. This is justified in the case of HIV/SIV/SHIV infection, where the parameter estimates are δ≈1.0/day and c≈20/day (16, 22).

Integrating

$$\frac{dT}{dt} = -\beta VT, \qquad \text{A 5}$$

and A 1 and A 3 from t=0 to t= t_P and using A 2 and A 4, we get the expression for virus peak

$$V_P = \frac{\delta}{c+\delta}V_0 + \frac{p}{c+\delta}T_0\left(1 - \frac{1}{R_0} - \frac{\ln R_0}{R_0}\right). \qquad \text{A 6}$$

Since $\delta<<p$, and the initial virus concentration in blood V_0 is usually much lower than T_0, the first term on the right hand side of A 6 can be neglected compared to the second term. The peak viral load then depends only on the constant parameters of the system (Figure 7a). Since $\delta<<c$, from A 6 we obtain the approximate expression for the virus peak

$$V_P = \frac{\delta}{\beta} R_0 \left(1 - \frac{1}{R_0} - \frac{\ln R_0}{R_0} \right). \quad \text{A 7}$$

Derivation of Eq. 11 for target cell minimum

In the infinite time limit all three derivatives Eq. 7-Eq. 9 must vanish. This means that the steady-state values of both V and I are zero, while the steady state value of target cells $T_{\min}$ is undetermined.

We can find $T_{\min}$ by integration. We substitute the expression for viral load from A 5,

$$V = -\frac{1}{\beta} \frac{d}{dt} \ln T, \quad \text{A 8}$$

into the second term on the right hand side of A 1, and integrate over time from zero to infinity. Taking into account that the infection is always cleared, i.e. that viral load vanishes in the long-time limit, we obtain the result

$$\int_0^\infty I dt = \frac{c}{\beta p} \ln \frac{T_0}{T_{\min}} - \frac{1}{p} V_0. \quad \text{A 9}$$

Next, we integrate both sides of A 3, and substitute the expression A 9 for the integral of infected cells. We note that the integral on the left hand side of A 3 vanishes at both limits (at t=0 and at t=∞), leading to

$$\beta \int_0^\infty V T dt = \frac{T_0}{R_0} \ln \frac{T_0}{T_{\min}} - \frac{\delta}{p} V_0. \quad \text{A 10}$$

After substituting A 10 into A 5 and integrating from 0 to ∞, we finally obtain the equation for $T_{\min}/T_0$,

$$\frac{T_{\min}}{T_0} - \frac{1}{R_0} \ln \frac{T_{\min}}{T_0} = 1. \quad \text{A 11}$$

In deriving A 11, we have again neglected the initial viral load in the inoculum ($V_0 \approx 0$).

Figure legends

Figure 1

Initial growth rates and decay rates after the peak viral load of SHIV-89.6P do not differ significantly between controls (black lines) and vaccinees (red lines).

Figure 2

(a) Timeline of virus growth and decay and (b) target cell decline in primary infection, obtained by numerical solution of Eq. 1-Eq. 3 and Eq. 7-Eq. 9. Full line – reduced model with λ, d_T=0, dashed line – standard model with λ=10 cells/μL/day, d_T =0.01 days^{-1}. The other parameters were β=8×10^{-8}mL/day, δ=0.8 day^{-1}, p=10^{3}μL/mL×500 copies/cell, c=20/day. The initial inoculum was 50 copies/mL. The dotted line in (b) represents the total (infected and uninfected) target cells in the standard model.

Figure 3

Target cell nadir T_{min} (full line) is lower than the steady state value T^* (dashed line) for all values of R_0.

Figure 4

(a) The curve describing the relationship between the logarithm of peak viral load and target cell depletion at the nadir has a universal S-shape, and only moves left or right with the change in log(δ/β). The constant δ/β is assumed to be characteristic of the virus type. Points higher on the same curve have higher basic reproductive ratio R_0. (b) The effect of lowering the virus peak by the same proportion on target cell depletion depends on the basic reproductive ratio corresponding to the viral load (i.e. on the value of δ/β, or the type of virus).

Figure 5

Best fit curves for the dependence of target cell depletion at the nadir on the peak of virus (from Eq. 10 and Eq. 11) (a) for SHIV-89.6P data (7, 25) (b) for SIV_{mac251} data (17, 18, 29). Full lines are the best fit curves obtained by optimization of the value of δ/β, and dashed lines are for the value of δ/β obtained by independent estimates, in Ref (7) for (a) and in Ref. (29) for (b).

Figure 6

Distribution of values of the basic reproductive ratio R_0 for SHIV-89.6P obtained from the initial exponential growth rate with fixed intracellular delay of 1 day for control (full circles) and vaccinated animals (full diamonds), and the values of the peak reproductive ratio R_P in the acute phase from virus peak and target cell nadir for control (open circles) and vaccinated animals (open diamonds). In the exponential growth phase, R_0 in controls and vaccines do not differ. However, R_P in controls is approximately 2 times higher than in vaccinees.

Figure 7

(a) Virus peak and (b) target cell nadir do not depend on the amount of virus in the inoculum (i.e. on initial condition), unless it is greater than the peak. Increasing the initial viral load only causes the peak/nadir to appear later.

Tables

	Exponential growth rate r_0		Virus decay rate	
	vaccinated	control	Vaccinated	control
mean	1.38	1.42	1.01	0.991
Standard error	0.043	0.055	0.046	0.058
95% CI	1.29-1.47	1.30-1.54	0.913-1.10	0.866-1.12
Mann-Whitney p-value	p=0.83		P=0.90	

Table 1

Initial exponential growth rate r_0 and decay rate of virus after the peak in vaccinated and unvaccinated animals are not significantly different.

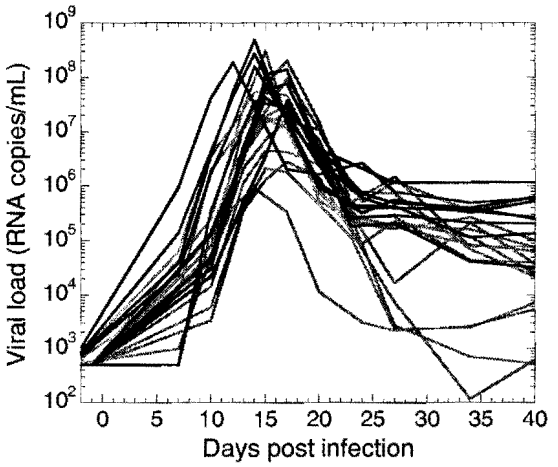

Figure 1

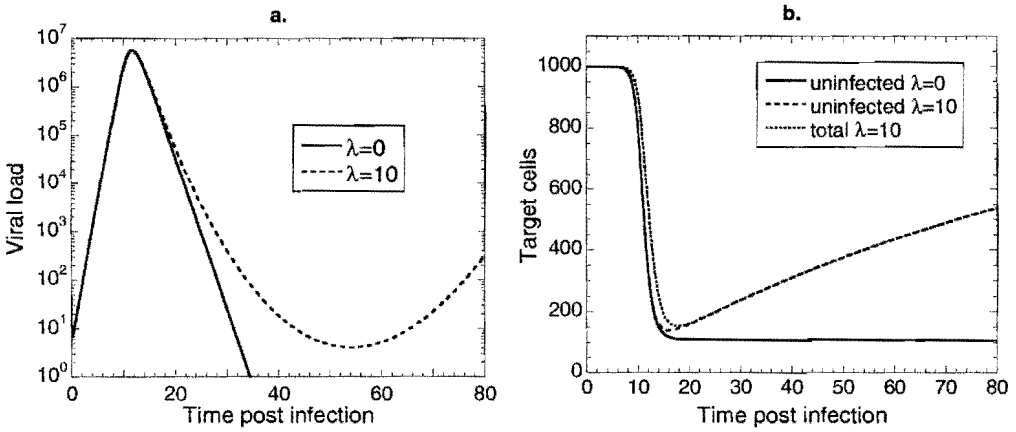

Figure 2

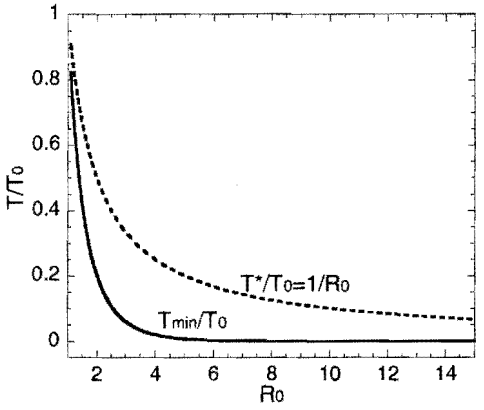

Figure 3

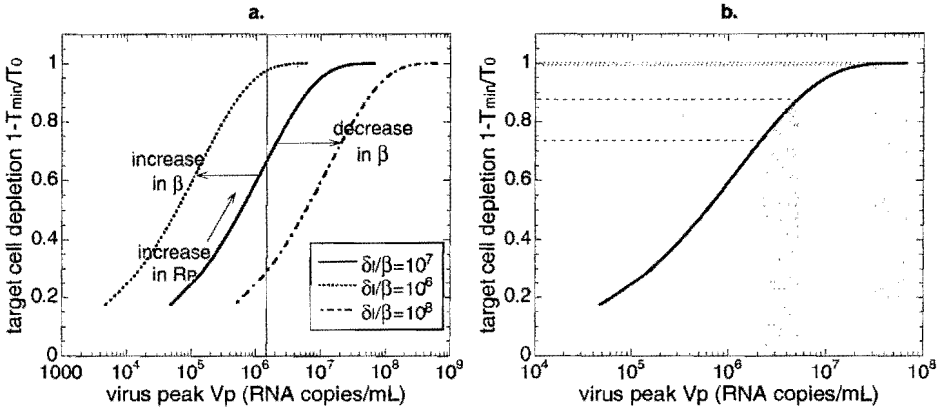

Figure 4

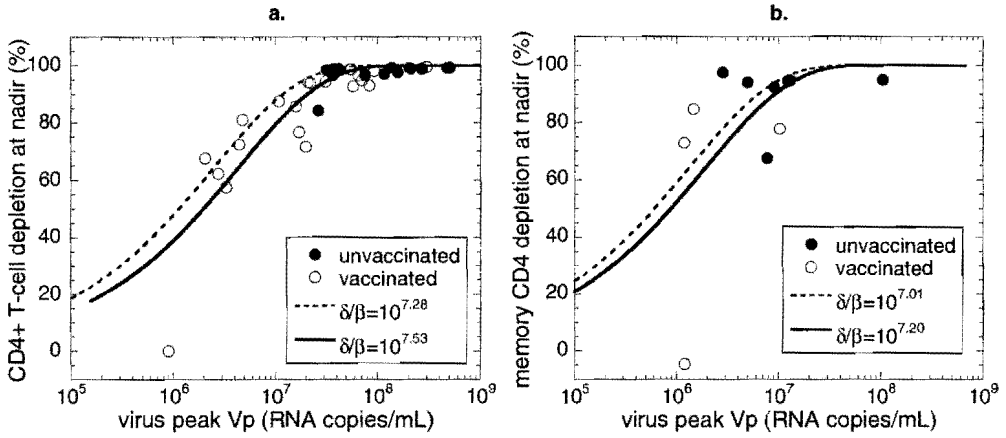

Figure 5

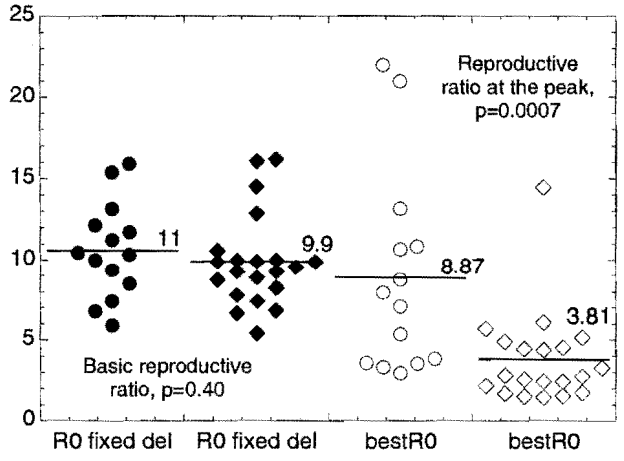

Figure 6

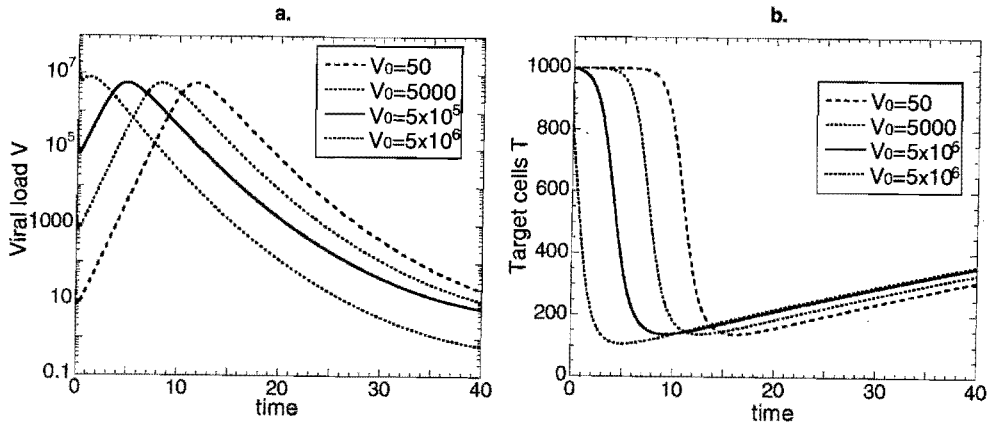
a.
b.
Viral load V
Target cells T
time
time
V0=50
V0=5000
V0=5x10^5
V0=5x10^6
10^7
10^5
1000
10
0.1
1000
800
600
400
200
0
0
10
20
30
40

Figure 7

References:

1. 2007. HIV vaccine failure prompts Merck to halt trial. Nature 449:390.
2. Brandin, E., R. Thorstensson, S. Bonhoeffer, and J. Albert. 2006. Rapid viral decay in simian immunodeficiency virus-infected macaques receiving quadruple antiretroviral therapy. J Virol 80:9861-4.
3. Chen, H. Y., M. Di Mascio, A. S. Perelson, D. D. Ho, and L. Zhang. 2007. Determination of virus burst size in vivo using a single-cycle SIV in rhesus macaques. Proc Natl Acad Sci U S A 104:19079-84.
4. Davenport, M. P., R. M. Ribeiro, and A. S. Perelson. 2004. Kinetics of virus-specific CD8+ T cells and the control of human immunodeficiency virus infection. Journal of Virology 78:10096-103.
5. Davenport, M. P., R. M. Ribeiro, L. Zhang, D. P. Wilson, and A. S. Perelson. 2007. Understanding the mechanisms and limitations of immune control of HIV. Immunol Rev 216:164-75.
6. Davenport, M. P., L. Zhang, A. Bagchi, A. Fridman, T. M. Fu, W. Schleif, J. W. Shiver, R. M. Ribeiro, and A. S. Perelson. 2005. High-potency human immunodeficiency virus vaccination leads to delayed and reduced CD8+ T-cell expansion but improved virus control. J Virol 79:10059-62.
7. Davenport, M. P., L. Zhang, J. W. Shiver, D. R. Casmiro, R. M. Ribeiro, and A. S. Perelson. 2006. Influence of peak viral load on the extent of CD4+ T-cell depletion in simian HIV infection. J Acquir Immune Defic Syndr 41:259-65.
8. Feinberg, M. B., and J. P. Moore. 2002. AIDS vaccine models: challenging challenge viruses. Nat Med 8:207-10.
9. Guadalupe, M., E. Reay, S. Sankaran, T. Prindiville, J. Flamm, A. McNeil, and S. Dandekar. 2003. Severe CD4+ T-cell depletion in gut lymphoid tissue during primary human immunodeficiency virus type 1 infection and substantial delay in restoration following highly active antiretroviral therapy. J Virol 77:11708-17.
10. Herz, A. V., S. Bonhoeffer, R. M. Anderson, R. M. May, and M. A. Nowak. 1996. Viral dynamics in vivo: limitations on estimates of intracellular delay and virus decay. Proceedings of the National Academy of Sciences of the United States of America 93:7247-51.
11. Ho, D. D., and Y. X. Huang. 2002. The HIV-1 vaccine race [Review]. Cell 110:135-138.
12. Ho, D. D., A. U. Neumann, A. S. Perelson, W. Chen, J. M. Leonard, and M. Markowitz. 1995. Rapid turnover of plasma virions and CD4 lymphocytes in HIV-1 infection. Nature 373:123-126.
13. Hockett, R. D., J. M. Kilby, C. A. Derdeyn, M. S. Saag, M. Sillers, K. Squires, S. Chiz, M. A. Nowak, G. M. Shaw, and R. P. Bucy. 1999. Constant mean viral copy number per infected cell in tissues regardless of high, low, or undetectable plasma HIV RNA. Journal of Experimental Medicine 189:1545-54.
14. Little, S. J., A. R. McLean, C. A. Spina, D. D. Richman, and D. V. Havlir. 1999. Viral dynamics of acute HIV-1 infection. Journal of Experimental Medicine 190:841-50.
15. Lloyd, A. L. 2001. The dependence of viral parameter estimates on the assumed viral life cycle: limitations of studies of viral load data. Proc Biol Sci 268:847-54.

16. Markowitz, M., M. Louie, A. Hurley, E. Sun, M. Di Mascio, A. S. Perelson, and D. D. Ho. 2003. A novel antiviral intervention results in more accurate assessment of human immunodeficiency virus type 1 replication dynamics and T-cell decay in vivo. J Virol 77:5037-8.
17. Mattapallil, J. J., D. C. Douek, A. Buckler-White, D. Montefiori, N. L. Letvin, G. J. Nabel, and M. Roederer. 2006. Vaccination preserves CD4 memory T cells during acute simian immunodeficiency virus challenge. J Exp Med 203:1533-41.
18. Mattapallil, J. J., D. C. Douek, B. Hill, Y. Nishimura, M. Martin, and M. Roederer. 2005. Massive infection and loss of memory CD4+ T cells in multiple tissues during acute SIV infection. Nature 434:1093-7.
19. Nowak, M. A., A. L. Lloyd, G. M. Vasquez, T. A. Wiltrout, L. M. Wahl, N. Bischofberger, J. Williams, A. Kinter, A. S. Fauci, V. M. Hirsch, and J. D. Lifson. 1997. Viral dynamics of primary viremia and antiretroviral therapy in simian immunodeficiency virus infection. Journal of Virology 71:7518-7525.
20. Nowak, M. A., and R. M. May. 2000. Virus dynamics: Mathematical principles of immunology and virology. Oxford University Press, Oxford.
21. Perelson, A. S., A. U. Neumann, M. Markowitz, J. M. Leonard, and D. D. Ho. 1996. HIV-1 dynamics in vivo: virion clearance rate, infected cell life-span, and viral generation time. Science 271:1582-6.
22. Ramratnam, B., S. Bonhoeffer, J. Binley, A. Hurley, L. Zhang, J. E. Mittler, M. Markowitz, J. P. Moore, A. S. Perelson, and D. D. Ho. 1999. Rapid production and clearance of HIV-1 and hepatitis C virus assessed by large volume plasma apheresis. Lancet 354:1782-5.
23. Reynolds, M. R., E. Rakasz, P. J. Skinner, C. White, K. Abel, Z. M. Ma, L. Compton, G. Napoe, N. Wilson, C. J. Miller, A. Haase, and D. I. Watkins. 2005. CD8+ T-lymphocyte response to major immunodominant epitopes after vaginal exposure to simian immunodeficiency virus: too late and too little. J Virol 79:9228-9235.
24. Ribeiro, R. M., N. M. Dixit, and A. S. Perelson. 2006. Modeling the *in vivo* growth rate of HIV:Implications for vaccination, p. 231-246. *In* R. Paton and L. A. McNamara (ed.), Multidiscpliniary approaches to theory in medicine. Elsevier, Amsterdam.
25. Shiver, J. W., T. M. Fu, L. Chen, D. R. Casimiro, M. E. Davies, R. K. Evans, Z. Q. Zhang, A. J. Simon, W. L. Trigona, S. A. Dubey, L. Huang, V. A. Harris, R. S. Long, X. Liang, L. Handt, W. A. Schleif, L. Zhu, D. C. Freed, N. V. Persaud, L. Guan, K. S. Punt, A. Tang, M. Chen, K. A. Wilson, K. B. Collins, G. J. Heidecker, V. R. Fernandez, H. C. Perry, J. G. Joyce, K. M. Grimm, J. C. Cook, P. M. Keller, D. S. Kresock, H. Mach, R. D. Troutman, L. A. Isopi, D. M. Williams, Z. Xu, K. E. Bohannon, D. B. Volkin, D. C. Montefiori, A. Miura, G. R. Krivulka, M. A. Lifton, M. J. Kuroda, J. E. Schmitz, N. L. Letvin, M. J. Caulfield, A. J. Bett, R. Youil, D. C. Kaslow, and E. A. Emini. 2002. Replication-incompetent adenoviral vaccine vector elicits effective anti-immunodeficiency-virus immunity. Nature 415:331-5.
26. Stafford, M. A., L. Corey, Y. Cao, E. S. Daar, D. D. Ho, and A. S. Perelson. 2000. Modeling plasma virus concentration during primary HIV infection. J Theor Biol 203:285-301.

27. **Staprans, S. I., P. J. Dailey, A. Rosenthal, C. Horton, R. M. Grant, N. Lerche, and M. B. Feinberg. 1999. Simian immunodeficiency virus disease course is predicted by the extent of virus replication during primary infection. J Virol 73:4829-39.**

28. **Wei, X., S. K. Ghosh, M. E. Taylor, V. A. Johnson, E. A. Emini, P. Deutsch, J. D. Lifson, S. Bonhoeffer, M. A. Nowak, B. H. Hahn, M. S. Saag, and G. M. Shaw. 1995. Viral dynamics in human immunodeficiency virus type 1 infection. Nature 373:117-122.**

29. **Wilson, D. P., J. J. Mattapallil, M. D. Lay, L. Zhang, M. Roederer, and M. P. Davenport. 2007. Estimating the infectivity of CCR5-tropic simian immunodeficiency virus SIV(mac251) in the gut. J Virol 81:8025-9.**